Available online at www.sciencedirect.com
SCIENCE DIRECT
Biochemical Pharmacology 70 (2005) 1096–1103
Biochemical Pharmacology
www.elsevier.com/locate/biochempharm

CYP2C-catalyzed delta(9)-tetrahydrocannabinol metabolism: Kinetics, pharmacogenetics and interaction with phenytoin

Tina M. Bland [a], Robert L. Haining [a], Timothy S. Tracy [b], Patrick S. Callery [a,*]

[a] *Department of Basic Pharmaceutical Sciences, School of Pharmacy, P.O. Box 9530, West Virginia University, 1 Medical Center Drive, Morgantown, WV 26506, USA*
[b] *Department of Experimental and Clinical Pharmacology, University of Minnesota, Minneapolis, MN 55455, USA*

Received 23 April 2005; accepted 8 July 2005

Abstract

delta(9)-Tetrahydrocannabinol (Δ^9-THC), the primary psychoactive constituent of marijuana, is subject to first pass hepatic metabolism primarily by hydroxylation to yield active and inactive oxygenated products. The primary metabolite is formed via oxidation of the allylic methyl group to yield 11-hydroxy-Δ^9-THC, which is oxidized further to 11-nor-9-carboxy-Δ^9-THC. The hydroxylation is thought to be mediated by CYP2C9. The present study was designed to address the kinetics and pharmacogenetics of CYP2C-mediated metabolism of (Δ^9)-THC by studying its metabolism in human liver microsomes and expressed enzymes. Expressed CYP2C9.1 exhibited high affinity for the hydroxylation of Δ^9-THC (apparent K_m, 2 μM), similar to that observed in human liver microsomes (apparent K_m, 0.8 μM). In contrast, the calculated intrinsic clearance (apparent V_m/K_m) for CYP2C9.2 and CYP2C9.3 was approximately 30% that of the wild type, CYP2C9.1. Given the high affinity of CYP2C9 for the hydroxylation of Δ^9-THC, we evaluated the potential for an interaction between Δ^9-THC, 11-hydroxy-Δ^9-THC, or 11-nor-9-carboxy-Δ^9-THC and the CYP2C9 substrate, phenytoin. Surprisingly, Δ^9-THC increased the rate of phenytoin hydroxylation in human liver microsomes and expressed CYP2C9 enzyme. Similar increases in rate were observed with co-incubation of 11-hydroxy-Δ^9-THC and 11-nor-9-carboxy-Δ^9-THC with phenytoin. These in vitro data suggest the potential for an interaction from the concomitant administration of Δ^9-THC and phenytoin that could result in decreased phenytoin concentrations in vivo.

Keywords: CYP2C; Tetrahydrocannabinol; Phenytoin; Drug interaction; Drug metabolism; Pharmacogenetics

1. Introduction

Marijuana remains one of the most widely abused illicit substances self-administered by both the oral and smoking routes. delta(9)-Tetrahydrocannabinol (Δ^9-THC), the principal psychoactive constituent found in the marijuana plant [1], is subject to first pass hepatic metabolism with the primary metabolite being formed by oxidation of the allylic methyl group to yield 11-hydroxy-Δ^9-THC (Fig. 1) [2]. Previous work with immunoinhibition methods and purified enzyme suggest that CYP2C9 is primarily responsible for the formation of the 11-hydroxy metabolite. However, kinetic studies were not performed and only a single substrate concentration (130 μM) was used to monitor metabolite formation [3]. CYP2C9 polymorphisms have been demonstrated to have profound effects on the rate of metabolism of several clinically important substrates [4–8]. Characterization of THC metabolism may lead to the discovery of clinically significant drug interactions associated with CYP2C9 polymorphisms. 11-Hydroxy-Δ^9-THC is the primary, rapidly formed THC metabolite that possesses psychoactive properties equal to that of the parent compound [9]. Thus, polymorphisms that show differing rates of formation of 11-hydroxy-Δ^9-THC are likely to alter the pharmacokinetic behavior of marijuana. To date, the effects of CYP450 polymorphisms on the hydroxylation of Δ^9-THC have not been adequately elucidated.

Given its widespread popularity, it is likely that marijuana is used concomitantly with other therapeutic agents. Drug–drug interactions, some severe, have been reported with marijuana and the concomitant administration of CYP2C9 substrates including tricyclic antidepressants [10] and fluoxetine [11]. More importantly, CYP2C9 metabolizes several narrow therapeutic index

* Corresponding author. Tel.: +1 304 293 1482; fax: +1 304 293 2576.
E-mail address: pcallery@hsc.wvu.edu (P.S. Callery).

0006-2952/$ – see front matter © 2005 Elsevier Inc. All rights reserved.
doi:10.1016/j.bcp.2005.07.007

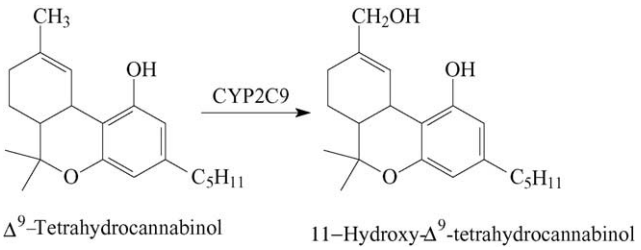

Fig. 1. Hepatic biotransformation of Δ^9-THC catalyzed by CYP2C9.

drugs, such as phenytoin. However, the potential for Δ^9-THC to alter drug metabolism or pharmacological effects has not been evaluated, despite the potential for co-administration.

The studies reported herein evaluate the contribution of cytochrome P450 isoforms to Δ^9-THC metabolism and determine the kinetics of 11-hydroxy-Δ^9-THC formation. Furthermore, the effects of CYP2C9 polymorphisms were evaluated as well as the potential for Δ^9-THC and its metabolites to interact with clinically important drugs, such as phenytoin.

2. Materials and methods

2.1. Chemicals and reagents

Methanol (Optima® grade), ammonium acetate, glacial acetic acid and THAM® [tris(hydroxymethyl)aminomethane] were obtained from Fisher Scientific Co. (Pittsburgh, PA). Ketoconazole, quinidine, furafylline, sulfaphenazole, 5,5-diphenylhydantoin (phenytoin), 5-(4-hydroxyphenyl)-5-phenylhydantoin (*p*HPPH), NADPH and dilauroylphosphatidylcholine were purchased from Sigma Chemical (St. Louis, MO). Δ^9-THC, 11-hydroxy-Δ^9-THC, 11-nor-9-carboxy-Δ^9-THC and $^2H_3$-11-hydroxy-Δ^9-THC (5,5,5-trideuteropentyl labeled) were purchased from Cerilliant (Round Rock, TX). 5-(3-Hydroxyphenyl)-5-phenylhydantoin (*m*HPPH) was purchased from Alltech (State College, PA). Human liver microsomes were obtained from the Liver Tissue Procurement and Distribution System (LTPADS) and protein levels determined by the method of Lowry et al. [12]. Additional pooled human liver microsomes and expressed CYP2C9.1, CYP2C9.2, CYP2C9.3 and CYP2C19 Supersomes® were obtained from BD BioSciences (Woburn, MA). Human CYP2C9.1, CYP2C8 and CYP2C18 and membrane preparations of CYP2C19 were expressed and purified according to previously established methods [13]. Cytochrome P450 concentration was determined by carbon monoxide difference spectroscopy by the method of Omura and Sato [14]. NADPH P450 reductase and cytochrome b5 were purchased from PanVera (Madison, WI).

2.2. Incubation conditions

Preliminary experiments showed linear conditions with respect to time and protein concentration for the conversion of Δ^9-THC to 11-hydroxy-Δ^9-THC. In all experiments, stock solutions of Δ^9-THC were diluted serially in methanol, and the final methanol concentration in the reaction mixture was 1.7%. The incubation mixtures containing either 20 μg of microsomal protein or 5 pmol cDNA-expressed CYP2C9.1, 10 pmol CYP2C9.2, 20 pmol CYP2C9.3 or 20 pmol CYP2C19 (both purified and membrane prepared), 50 mM THAM® pH 7.4 and Δ^9-THC (0.25–20 μM) were prewarmed for 5 min at 37 °C. Reactions were initiated by adding NADPH yielding a final concentration of 1 mM, and the reaction mixtures (200 μL total volume) were incubated for 5 min at 37 °C. Reactions were quenched by adding 30 μL of glacial acetic acid and placing the incubation tubes on ice. After the addition of 10 ng of $^2H_3$-11-hydroxy-Δ^9-THC as internal standard, the mixtures were centrifuged at 10,000 rpm for 4 min and 20 μL aliquots of the supernatant injected onto the HPLC system.

2.3. Cytochrome P450 inhibition studies

The effects of the cytochrome P450 inhibitors sulfaphenazole (CYP2C9), quinidine (CYP2D6), ketoconazole (CYP3A4) and furafylline (CYP1A2) on the kinetics of Δ^9-THC conversion to 11-hydroxy-Δ^9-THC were investigated in human liver microsomes. A preincubation period of 15 min was used for the mechanism-based inhibitor, furafylline. Various concentrations of inhibitors were incubated with Δ^9-THC as described above and the production of 11-hydroxy-Δ^9-THC formation was determined. The inhibitors were chosen on the basis of selective inhibition of a particular cytochrome P450 enzyme and the concentrations used had been previously established [15].

2.4. Drug–drug interaction studies

Preliminary experiments were conducted to determine the linear range with respect to incubation time and protein concentrations for the conversion of phenytoin to *p*HPPH. In all experiments, stock solutions of all drugs used were diluted serially in methanol, and the final methanol concentration in the reaction mixture was 1.7%. The incubation mixtures containing either 150 μg of microsomal protein or 20 pmol of cDNA-expressed CYP2C9.1, 50 mM THAM® pH 7.4, phenytoin (2–200 μM) and effector. Effector solutions consisting Δ^9-THC (5 nM–2 μM), 11-hydroxy-Δ^9-THC (100–500 nM), 11-nor-9-carboxy-Δ^9-THC (100–500 nM), dapsone (0.1–100 μM), sulfaphenazole (10 μM) and lansoprazole [16] (50 μM) were prewarmed for 5 min at 37 °C. All concentrations listed represent final concentrations in the incubation vessel unless otherwise noted. Reactions were initiated by adding

NADPH to give a final concentration of 1 mM, and the reaction mixtures (200 μL total volume) were incubated for 30 min at 37 °C. Reactions were quenched with 40 μL of mobile phase (40:60 MeOH:0.5% glacial acetic acid) and placing the incubation tubes on ice. The mixtures were then centrifuged at 10,000 rpm for 4 min, and 20 μL aliquots of the supernatant were injected onto an HPLC system. For incubation mixtures using cDNA-expressed CYP2C9.1, the enzyme was reconstituted in dilauroylphosphatidyl choline vesicles in the presence of P450 reductase and cytochrome b5 in a 1:2:1 ratio. For experiments with CYP2C9.2 and CYP2C9.3 Supersomes®, 20 pmol of enzyme was used with a single phenytoin concentration (50 μM) and a single effector concentration (50 nM). Otherwise, the incubations were performed as previously described.

2.5. Analytical procedures

The separation and detection system consisted of a Waters Alliance® 2690XE HPLC system coupled to a Waters Micromass ZMD mass spectrometer programmed to utilize electrospray ionization in positive ion mode with select ion recording. For 11-hydroxy-Δ^9-THC analysis, the mobile phase consisted of methanol:10 mM ammonium acetate, pH 4.0 (85:15, v/v) pumped at 0.2 mL/min through a Waters YMC Pro C_{18} 2.0 mm × 50 mm reversed phase column at ambient temperature. Under these conditions, 11-hydroxy-Δ^9-THC (*m*/*z* 331) and Δ^9-THC (*m*/*z* 315) were eluted within 5 min with retention times of approximately 2.4 and 3.4 min, respectively. $^2H_3$-11-hydroxy-Δ^9-THC eluted at the same time as 11-hydroxy-Δ^9-THC and was detected at *m*/*z* 334. This assay was validated in our laboratory with regard to both between day and within day precision and accuracy. The precision of the assay was 8.2% or less and the accuracy varied within −9.9 and 4.8% of the nominal concentration. Separation of monohydroxylated metabolites formed from incubation with CYP2C19 was performed as described above with the following exceptions: the mobile phase consisted of methanol:0.5% glacial acetic acid (40:60, v/v) pumped at 0.2 mL/min through a Waters YMC Pro C_8 2.0 mm × 50 mm reversed phase column at 30 °C for 5 min followed by a 35 min gradient elution in which the methanol concentration was increased in a linear fashion from 5 to 35 min to a maximum of 90% final methanol concentration followed by an immediate return to starting conditions. The system was then equilibrated for 8 min prior to the next sample injection. Under these conditions, 11-hydroxy-Δ^9-THC and an additional monohydroxylated metabolite were resolved with baseline separation and retention times of approximately 31 and 29 min, respectively. For *p*HPPH formation, the mobile phase consisted of methanol–0.5% glacial acetic acid (40:60, v/v) pumped at 0.2 mL/min through a Waters YMC Pro C_8 2.0 mm × 50 mm reversed phase column at ambient temperature. *p*HPPH (*m*/*z* 269) and phenytoin (*m*/*z* 253) exhibited retention times of approximately 2.9 and 6 min, respectively. Separation of *p*HPPH and *m*HPPH was achieved using an isocratic mobile phase consisting of methanol:0.25% acetic acid (28:72) pumped at 0.2 mL/min. *p*HPPH and *m*HPPH were separated within 12 min with retention times of approximately 7.5 and 9.3 min, respectively.

2.6. Data analysis

Unless otherwise stated, all results are presented as the mean of at least 3 separate experiments. A standard Michaelis–Menten model was fit to the data evaluating the formation of metabolite from Δ^9-THC using Sigma-Plot® 2001 (SPSS Software, Chicago, IL) and determinations of apparent K_m and V_m values were obtained. Additionally, kinetic parameters for the formation of metabolite from THC were estimated using a substrate inhibition model to fit the data according to Eq. (1): $v = \frac{V_m}{1+\frac{K_m}{S}+\frac{S}{K_i}}$ where K_i represents the binding constant for the drug molecule at the inhibitory site of the enzyme. All data fitting was performed using Sigma-Plot® 7.0 (SPSS Inc.) and appropriateness of the fits determined by examination and comparison of the residuals, residual sum of squares, coefficients of determination and F values.

3. Results

3.1. Kinetics of Δ^9-THC hydroxylation in human liver microsomes

The conversion of Δ^9-THC to 11-hydroxy-Δ^9-THC can be described using the Michaelis–Menten model (Fig. 2) within the range of concentrations up to 20 μM. At concentrations higher than 20 μM, a decrease in reaction velocity was observed (Fig. 2 inset shows data for 11-hydroxy-Δ^9-THC formation over a range of concentrations that produced substrate inhibition). Kinetic parameter estimates from both models are presented in Table 1.

3.2. CYP isoform involvement in Δ^9-THC metabolism in human liver microsomes

To determine the involvement of other CYP isoforms in Δ^9-THC (2 μM) metabolism, a battery of specific inhibitors was utilized including: ketoconazole (CYP3A4), quinidine (CYP2D6), furafylline (CYP1A2) and sulfaphenazole (CYP2C9). Inhibition of Δ^9-THC 11-hydroxylation by sulfaphenazole and ketoconazole are presented in Fig. 3A and B. Δ^9-THC metabolism was clearly inhibited by co-incubation with sulfaphenazole further verifying that CYP2C9 is, at least in part, responsible for the conversion of Δ^9-THC to 11-hydroxy-Δ^9-THC. Slight inhibition of Δ^9-THC metabolism was observed at high concentrations of ketoconazole (20 μM), most likely due to the nonselectivity of ketoco-

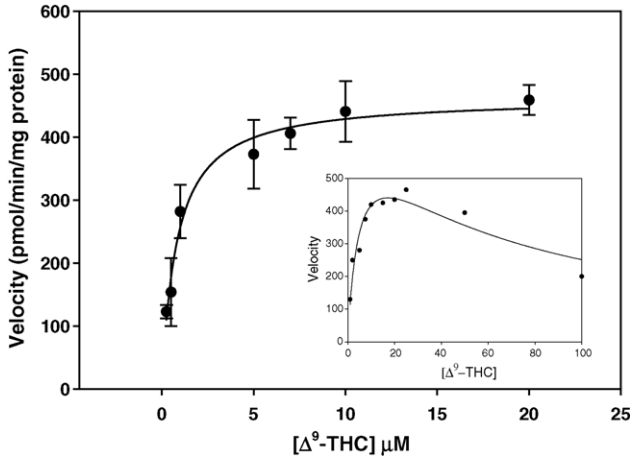

Fig. 2. Δ^9-THC hydroxylation in human liver microsomes: data points represent the mean (n = 3) with error bars representing standard deviations. A Michaelis–Menten model was fit to the data. Kinetic parameter estimates for the fit can be observed in Table 1. (*Inset*) Data for 11-hydroxy-Δ^9-THC formation over a range of substrate concentrations that produced substrate inhibition. A substrate inhibition model (Eq. (1)) was used to fit the data and estimates of the kinetic parameters, K_m, V_m and K_i can be observed in Table 1.

nazole in inhibiting both CYP2C9 and CYP3A4 at higher concentrations [17]. Δ^9-THC metabolism was not inhibited upon co-incubation with either quinidine or furafylline (data not shown), suggesting that neither CYP2D6 nor CYP1A2 are involved in the 11-hydroxylation of Δ^9-THC.

3.3. Pharmacogenetic influences on Δ^9-THC metabolism by CYP2C9

The hydroxylation of Δ^9-THC was investigated with expressed CYP2C9.1 (Arg_{144}), CYP2C9.2 (Cys_{144}) and CYP2C9.3 (Leu_{359}). The conversion of Δ^9-THC to 11-hydroxy-Δ^9-THC was described by Michaelis–Menten kinetics and the apparent kinetic constants were estimated using Δ^9-THC concentrations up to 20 μM in CYP2C9.1.

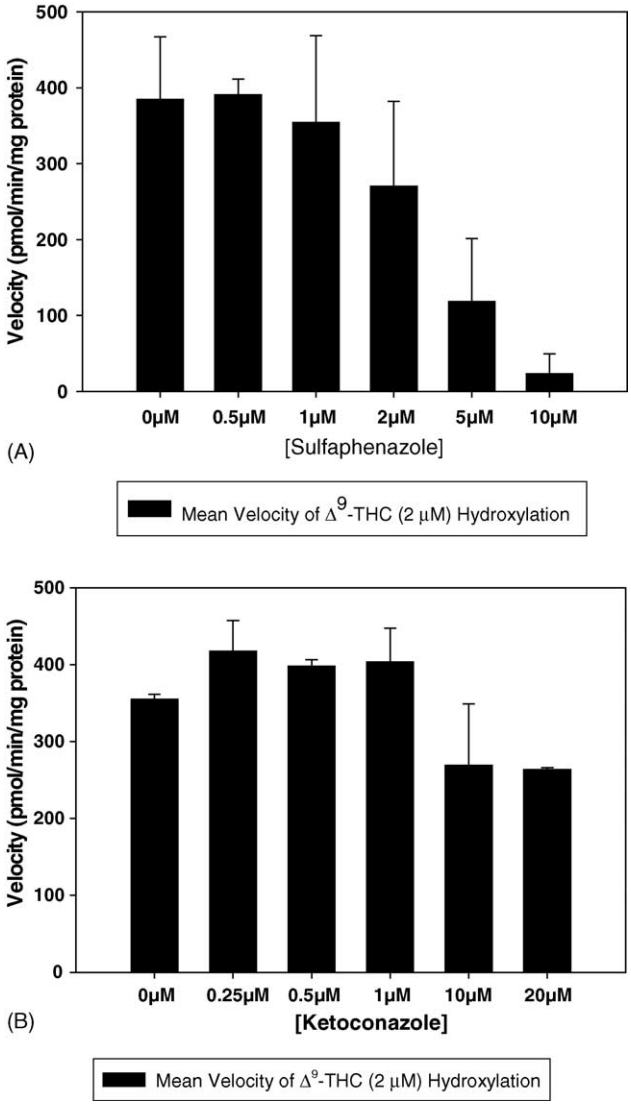

Fig. 3. (A) Inhibition of Δ^9-THC (2 μM) hydroxylation in human liver microsomes by sulfaphenazole (0–10 μM). (B) Inhibition of Δ^9-THC (2 μM) hydroxylation in human liver microsomes by ketoconazole (0–20 μM).

Table 1
Kinetic constants for 11-hydroxy-Δ^9-THC formation

	K_m [a] (S.E.)	V_m [b] (S.E.)	CL_{int} [c]	K_i [a] (S.E.)
Human liver microsomes[d]	0.80 (0.12)	463[e] (15)	nd[f]	na[g]
Human liver microsomes[h]	5.20 (2.00)	706[e] (127)	nd[f]	57 (25)
CYP2C9.1	2.13 (0.41)	6.39[f] (0.32)	3.0	
CYP2C9.2	11.10 (1.53)	10.11[f] (0.40)	0.9	
CYP2C9.3	6.69 (1.70)	5.36[f] (0.34)	0.8	

[a] μM.
[b] Units for V_m are different depending on the enzyme preparation used (human liver microsomes vs. expressed enzyme).
[c] μL/(min pmol P450).
[d] Michaelis–Menten model used to fit the data.
[e] pmol/(min mg protein).
[f] Not determined.
[g] Not applicable.
[h] A substrate inhibition model (Eq. (1)) used to fit the data.

As observed with human liver microsomal preparations, incubation of CYP2C9.1 at concentrations of Δ^9-THC higher than 20 μM resulted in substrate inhibition as illustrated by a decrease in reaction velocity (data not shown). Higher concentrations of Δ^9-THC were required to reach saturation in both CYP2C9.2 and CYP2C9.3 and the apparent kinetic constants were estimated using Δ^9-THC concentrations up to 200 μM, with no apparent substrate inhibition noted in these variant isoforms. Mean velocity versus substrate concentration curves for each CYP2C9 variant are depicted in Figs. 4 and 5 and the resulting kinetic parameter estimates are presented in Table 1. Expressed CYP2C9.1 exhibits high affinity for the hydroxylation of Δ^9-THC (apparent K_m of 2 μM), similar to that observed in human liver microsomes (apparent K_m of 0.8 μM). With respect to enzyme efficiency, the

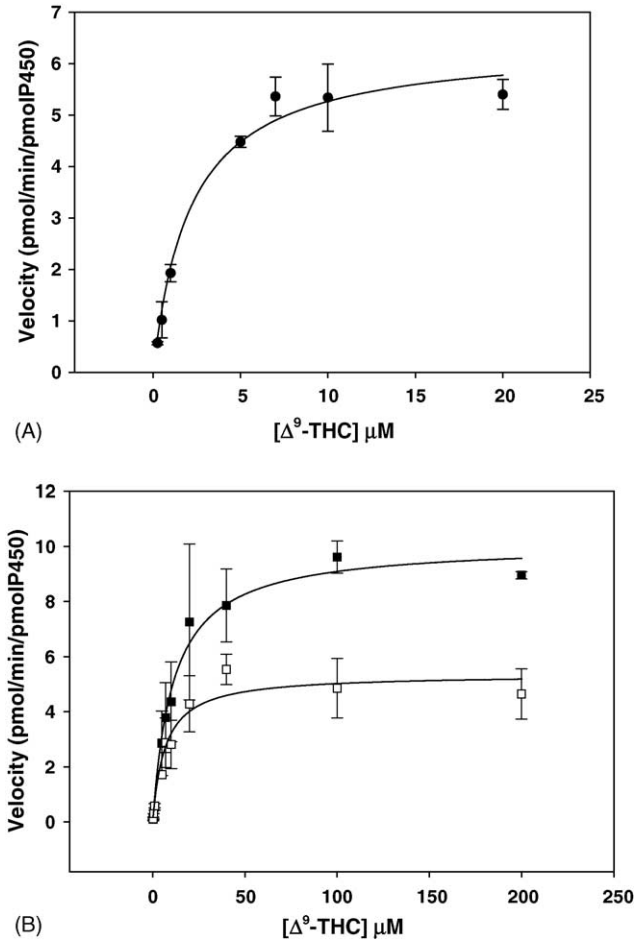

Fig. 4. (A) Δ^9-THC hydroxylation in CYP2C9.1 expressed enzyme. Data points represent the mean ($n = 3$) with error bars representing standard deviations. A Michaelis–Menten model was fit to the data. Kinetic parameter estimates for the fit can be observed in Table 1. (B) Δ^9-THC hydroxylation in CYP2C9.2 (■) and CYP2C9.3 (□) expressed enzyme. Data points represent the mean ($n \geq 3$) incubations with error bars representing standard deviations. A Michaelis–Menten model was fit to the data. Kinetic parameter estimates for the fit can be observed in Table 1.

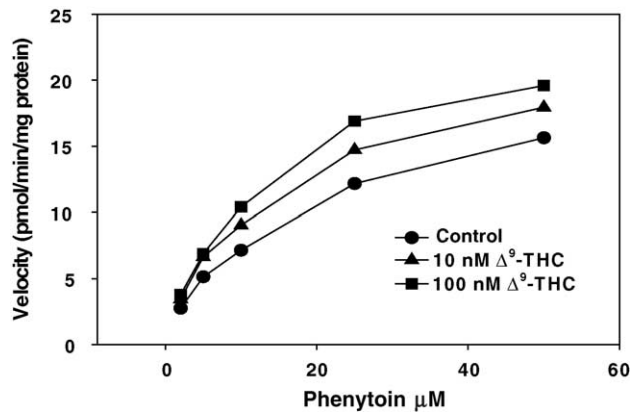

Fig. 5. Phenytoin hydroxylation in human liver microsomes in the presence and absence of Δ^9-THC: data points represent the mean ($n \geq 3$). The standard error was less than 15% of the mean.

calculated intrinsic clearance (apparent V_m/K_m) for CYP2C9.2 and CYP2C9.3 was approximately 30% that of the wild-type CYP2C9.1 enzyme.

3.4. Incubation of Δ^9-THC with CYP2C19, CYP2C18 and CYP2C8

The hydroxylation of Δ^9-THC was investigated with expressed CYP2C19, CYP2C18 and CYP2C8. Preliminary experiments indicate that CYP2C19 catalyzed the conversion of Δ^9-THC to 11-hydroxy-Δ^9-THC and an additional co-eluting metabolite (*m/z* 331), the structure of which remains to be determined. Experiments to further investigate the contribution of CYP2C19 to the metabolism of Δ^9-THC are in process. Neither CYP2C18 nor CYP2C8 catalyzed the formation of 11-hydroxy-Δ^9-THC under the experimental conditions tested.

3.5. Assessment of potential for Δ^9-THC and metabolites to interact with CYP2C9 substrates

To assess the potential for drug interactions involving Δ^9-THC and its 11-hydroxy and 11-nor-9-carboxy metabolites with a common CYP2C9 substrate, phenytoin aromatic hydroxylation by both human liver microsomal preparations and expressed CYP2C9, were evaluated in the presence of these compound.

In the case of phenytoin hydroxylation, samples were analyzed for production of the *para*-hydroxylated metabolite (*p*HPPH) and the *meta*-metabolite, 5-(3-hydroxyphenyl)-5-phenylhydantoin (*m*HPPH). Analytical methods as outlined above allowed baseline separation of the chromatograms representing the *para*- and *meta*-hydroxylated metabolites of phenytoin; however, under the conditions tested, only the *para*-hydroxylated metabolite was formed. The effect of Δ^9-THC (5–500 nM) on the rate of *p*HPPH formation in human liver microsomes is presented in Fig. 5. Surprisingly, Δ^9-THC activated the human liver microsomal metabolism of phenytoin, represented by an apparent increase in velocity, compared to control. Comparable changes in velocity were noted in expressed CYP2C9 enzyme systems, confirming the involvement of CYP2C9 (data not shown). Interestingly, the prototype CYP2C9 activator, dapsone [18], had no effect on phenytoin hydroxylation (data not shown). Conversely, lansoprazole [16], a known CYP2C activator, produced substantial activation of phenytoin metabolism (~1200%) (data not shown). Phenytoin had little effect on the conversion of Δ^9-THC to 11-hydroxy-Δ^9-THC in human liver microsomes (data not shown). Consistent with the effects observed with Δ^9-THC, both 11-hydroxy-Δ^9-THC and 11-nor-9-carboxy-Δ^9-THC activated phenytoin hydroxylation in human liver microsomes (Fig. 6). The CYP2C9.2 and CYP2C9.3 variants were also tested at single substrate (phenytoin) and single effector (Δ^9-THC, 11-hydroxy-Δ^9-THC or 11-nor-9-carboxy-Δ^9-

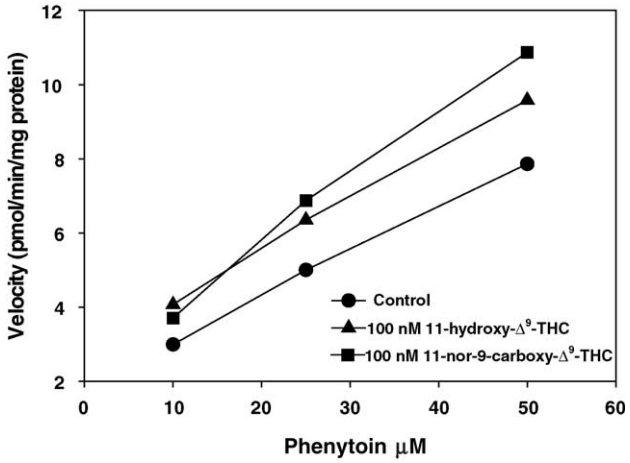

Fig. 6. Phenytoin hydroxylation in human liver microsomes in the presence and absence of 11-hydroxy-Δ^9-THC or 11-nor-9-carboxy-Δ^9-THC: data points represent the mean ($n \geq 3$). The standard error was less than 15% of the mean.

THC) concentrations for activation of phenytoin hydroxylation. Activation was observed for the CYP2C9.2 variant with parent THC as well as both metabolites and the degree of activation was comparable to that observed in human liver microsomes. Formation of *p*HPPH in samples incubated with CYP2C9.3 and phenytoin alone were below the limit of quantitation (LOQ), but in samples incubated with both substrate and effector, activation was apparent as the formation of *p*HPPH was greater than control samples and above the LOQ (data not shown). Thus, estimation of percent activation was not possible.

4. Discussion

Δ^9-THC in humans is metabolically converted to several metabolites, of which the primary metabolite, 11-hydroxy-Δ^9-THC, also contributes to its psychotropic activity [3]. However, little information is available concerning the kinetics of this reaction or the effect of genetic polymorphisms on this process. The present work describes the kinetics of conversion of Δ^9-THC to 11-hydroxy-Δ^9-THC catalyzed by CYP2C9.1 (wild-type) and two variant isoforms. Additionally, it was discovered that CYP2C19 may also play a role in the formation of 11-hydroxy-Δ^9-THC and forms an additional metabolite (presumably, monohydroxylated) that has not been fully characterized. Finally, it was observed that Δ^9-THC and its 11-hydroxy and 11-nor-9-carboxy metabolites are capable of activating phenytoin *para*-hydroxylation.

In the present studies, expressed CYP2C9.1 (wild-type) exhibited a high affinity for the hydroxylation of Δ^9-THC (apparent K_m, 2 μM), similar to that observed in human liver microsomes (apparent K_m, 1 μM). Specifically, a calculated intrinsic clearance of 3 μL/(min pmol P450) was observed in wild-type enzyme. These findings along with the substantial inhibition of metabolite formation in the presence of sulfaphenazole, extend the findings of Bornheim et al. [3] demonstrating that CYP2C9 is efficient at metabolizing Δ^9-THC and is likely the primary enzyme involved in the 11-hydroxylation reaction.

To further assess whether other CYP2C isoforms may play a role in the metabolism of Δ^9-THC, additional experiments were conducted with expressed enzymes, particularly CYP2C19. Despite the fact that CYP2C9 and CYP2C19 are very similar in amino acid sequence, these two enzymes have very distinctive substrate specificities. CYP2C19 appears to be less sterically hindered in its active site compared to CYP2C9 as it metabolizes both (*R*)- and (*S*)-warfarin at multiple sites (4′, 6, 7 and 8 positions) and hydroxylates both the pro-(*S*) and pro-(*R*) rings of phenytoin. CYP2C9 is more selective in that it catalyzes the conversion of (*S*)-warfarin to the 6- and 7-hydroxy metabolites and prefers the pro-(*S*) ring of phenytoin [19–21]. In the present studies, we found that CYP2C19 catalyzed the conversion of Δ^9-THC to both 11-hydroxy-Δ^9-THC and, to a lesser extent, an isomeric metabolite of the same molecular weight as 11-hydroxy-Δ^9-THC. This finding suggests that the contribution of CYP2C19 to the metabolism of Δ^9-THC warrants further investigation.

Single nucleotide polymorphisms in the CYP2C9 gene have been associated with interindividual and ethnic differences in the pharmacokinetic profiles of various CYP2C9 substrates. Several allelic variants of CYP2C9 have been reported with the most extensively described being CYP2C9.2 and CYP2C9.3. Both of these variants are present in the Caucasian population with an allelic frequency in the range of 0.08–0.14 for CYP2C9.2 and 0.04–0.16 for CYP2C9.3. In people of African descent, both variants are much less common, and in the Asian population, CYP2C9.2 has not been detected to date [22–28]. Until now, the metabolism of Δ^9-THC in CYP2C9 variants had not been evaluated. In comparison to wild-type enzyme, higher apparent V_m and K_m estimates were observed with CYP2C9.2-mediated catalysis of Δ^9-THC yielding a calculated intrinsic clearance of 0.9 μL/(min · pmol P450). Likewise, CYP2C9.3 mediated metabolism of Δ^9-THC yielded essentially no change in apparent V_m, but did show an increase in apparent K_m which resulted in a calculated intrinsic clearance of 0.7 μL/(min pmol P450). Our results demonstrate that the enzyme efficiency for CYP2C9.2 and CYP2C9.3 is about one third that of the wild-type CYP2C9.1, respectively, suggesting that individuals with these polymorphisms would experience altered rates of Δ^9-THC 11-hydroxylation. However, the pharmacological consequences of this are difficult to predict since both the parent compound and the 11-hydroxy metabolite possess psychotropic properties.

Because the low K_m estimate of CYP2C9 implies high enzyme affinity, we investigated the drug-drug interaction potential of Δ^9-THC and its 11-hydroxy and 11-nor-9-

carboxy metabolites with the prototypical CYP2C9 substrate, phenytoin. Activation of phenytoin metabolism was demonstrated in human liver microsomal and expressed CYP2C9.1 preparations when co-incubated with Δ^9-THC and its two primary metabolites at clinically relevant concentrations. The apparent velocity of the reaction was increased through coincubation with Δ^9-THC and its 11-hydroxy and 11-nor-9-carboxy metabolites. However, because the effector (Δ^9-THC) concentration is likely changing over the 30-min incubation necessary for adequate *p*HPPH formation, these data were not evaluated further.

Effector (Δ^9-THC and metabolites) concentrations were initially chosen based on in vivo plasma drug concentrations expected following marijuana administration (~200 ng/mL; 600 nM at C_{max}) and increased up to the apparent K_m (~2 μM). Within this concentration, activation of phenytoin metabolism appeared to be maximal and thus, lower concentrations were explored in an attempt to define a concentration–response relationship. For Δ^9-THC (5–500 nM), activation of phenytoin metabolism followed an effector–concentration dependent relationship spanning no effect to maximal activation. For 11-hydroxy-Δ^9-THC and the carboxy-metabolite of Δ^9-THC, a 10-fold higher concentration of effector (100 nM) was required to reach activation levels comparable to that observed with Δ^9-THC. Thus, activation of CYP2C9 by Δ^9-THC and its metabolites appears to occur at concentrations lower than previously observed with dapsone [29], comparable to those previously reported with amiodarone [30], but less than reported with lansoprazole [16].

Interactions between substrates and inhibitors or activators of cytochromes P450 are complex and difficult to predict given the differential effects that may be observed depending on the substrate studied and the isoforms involved. For example, commonly used substrates of CYP3A4 exhibit substrate-dependent drug–drug interactions characterized as mutual inhibition, partial inhibition and activation that can be explained by the concurrent binding to the active site by multiple substrates or ligands [31]. The involvement of multiple binding sites may result in an inhibitory or stimulatory effect at only one site or a differential effect at each site, thus complicating a direct prediction of a potential in vivo interaction. Taking into consideration hydrogen bond acceptor and hydrophobic properties, a predictive model for linking in vitro heteroactivation for specific pairs of effectors and substrates has been developed for CYP3A4 [32].

Our in vitro data suggest the potential for an interaction from the concomitant administration of Δ^9-THC and phenytoin that could result in decreased phenytoin concentrations in vivo resulting from an increased rate of phenytoin metabolite formation observed in the presence of not only Δ^9-THC, but also its two primary metabolites. To our knowledge, this is the first observation of a commonly abused illicit substance serving to activate the in vitro metabolism of a widely prescribed medication. For drugs, such as phenytoin, in which the efficacy and toxicity depend on maintenance of plasma concentrations within a narrow range, the ability to accurately predict drug–drug interactions becomes vital for patient safety. Another factor to consider in estimating the clinical relevance of the activation phenomenon is the unbound fraction of drug, since phenytoin, THC and THC metabolites are highly protein bound [33,34]. In vivo studies are needed to determine if the THC–phenytoin interaction observed in vitro is a clinically relevant drug–drug interaction.

Acknowledgements

This work was supported in part by NIH Grants #GM63215 to T.S.T., #N01-DK-6-2274 to the Liver Tissue Procurement and Distribution System and award number 2001-RC-CX-K013 to P.S.C. from the Office of Justice Programs, National Institute of Justice, Department of Justice. Points of view in this document are those of the authors and do not necessarily represent the official position of the U.S. Department of Justice.

References

[1] Gaoni Y, Mechoulam R. Isolation, structure and partial synthesis of an active constituent of hashish. J Am Chem Soc 1964;86:1646–7.
[2] Wall ME, Sadler BM, Brine D, Taylor H, Perez-Reyes M. Metabolism, disposition, and kinetics of delta-9-tetrahydrocannabinol in men and women. Clin Pharmacol Ther 1983;34:352–63.
[3] Bornheim LM, Lasker JM, Raucy JL. Human hepatic microsomal metabolism of delta 1-tetrahydrocannabinol. Drug Metab Dispos 1992;20:241–6.
[4] Rettie AE, Wienkers LC, Gonzalez FJ, Trager WF, Korzekwa KR. Impaired (*S*)-warfarin metabolism catalysed by the R144C allelic variant of CYP2C9. Pharmacogenetics 1994;4:39–42.
[5] Steward DJ, Haining RL, Henne KR, Davis G, Rushmore TH, Trager WF, et al. Genetic association between sensitivity to warfarin and expression of CYP2C9*3. Pharmacogenetics 1997;7:361–7.
[6] Kidd RS, Curry TB, Gallagher S, Edeki T, Blaisdell J, Goldstein JA. Identification of a null allele of CYP2C9 in an African–American exhibiting toxicity to phenytoin. Pharmacogenetics 2001;11:803–8.
[7] Kirchheiner J, Brockmoller J, Meineke I, Bauer S, Rohde W, Meisel C, et al. Impact of CYP2C9 amino acid polymorphisms on glyburide kinetics and on the insulin and glucose response in healthy volunteers. Clin Pharmacol Ther 2002;71:286–96.
[8] Tracy TS, Hutzler JM, Haining RL, Rettie AE, Hummel MA, Dickmann LJ. Polymorphic variants (CYP2C9*3 and CYP2C9*5) and the F114L active site mutation of CYP2C9: effect on atypical kinetic metabolism profiles. Drug Metab Dispos 2002;30:385–90.
[9] Hollister LE, Gillespie HK. Action of delta-9-tetrahydrocannabinol. An approach to the active metabolite hypothesis. Clin Pharmacol Ther 1975;18:714–9.
[10] Wilens TE, Biederman J, Spencer TJ. Case study: adverse effects of smoking marijuana while receiving tricyclic antidepressants. J Am Acad Child Adolesc Psychiatry 1997;36:45–8.
[11] Stoll AL, Cole JO, Lukas SE. A case of mania as a result of fluoxetine–marijuana interaction. J Clin Psychiatry 1991;52:280–1.

[12] Lowry OH, Rosebrough NJ, Farr AL, Randall RJ. Protein measurement with the Folin phenol reagent. J Biol Chem 1951;193:265–75.
[13] Haining RL, Hunter AP, Veronese ME, Trager WF, Rettie AE. Allelic variants of human cytochrome P450 2C9: baculovirus-mediated expression, purification, structural characterization, substrate stereoselectivity, and prochiral selectivity of the wild-type and I359L mutant forms. Arch Biochem Biophys 1996;333:447–58.
[14] Omura T, Sato R. The carbon monoxide-binding pigment of liver microsomes. II. Solubilzation, purification, and properties. J Biol Chem 1964;239:2379–85.
[15] Bjornsson TD, Callaghan JT, Einolf HJ, Fischer V, Gan L, Grimm S, et al. The conduct of in vitro and in vivo drug–drug interaction studies: a Pharmaceutical Research and Manufacturers of America (PhRMA) perspective. Drug Metab Dispos 2003;31:815–32.
[16] Liu KH, Kim MJ, Jung WM, Kang W, Cha IJ, Shin JG. Lansoprazole enantiomer activates human liver microsomal CYP2C9 catalytic activity in a stereospecific and substrate-specific manner. Drug Metab Dispos 2005;33:209–13.
[17] Zhang W, Ramamoorthy Y, Kilicarslan T, Nolte H, Tyndale RF, Sellers EM. Inhibition of cytochromes P450 by antifungal imidazole derivatives. Drug Metab Dispos 2002;30:314–8.
[18] Hutzler JM, Hauer MJ, Tracy TS. Dapsone activation of CYP2C9-mediated metabolism: evidence for activation of multiple substrates and a two-site model. Drug Metab Dispos 2001;29:1029–34.
[19] Bajpai M, Roskos LK, Shen DD, Levy RH. Roles of cytochrome P4502C9 and cytochrome P4502C19 in the stereoselective metabolism of phenytoin to its major metabolite. Drug Metab Dispos 1996;24:1401–3.
[20] Kaminsky LS, de Morais SM, Faletto MB, Dunbar DA, Goldstein JA. Correlation of human cytochrome P4502C substrate specificities with primary structure: warfarin as a probe. Mol Pharmacol 1993;43:234–9.
[21] Rettie AE, Korzekwa KR, Kunze KL, Lawrence RF, Eddy AC, Aoyama T, et al. Hydroxylation of warfarin by human cDNA-expressed cytochrome P-450: a role for P-4502C9 in the etiology of (*S*)-warfarin-drug interactions. Chem Res Toxicol 1992;5:54–9.
[22] Dickmann LJ, Rettie AE, Kneller MB, Kim RB, Wood AJ, Stein CM, et al. Identification and functional characterization of a new CYP2C9 variant (CYP2C9*5) expressed among African Americans. Mol Pharmacol 2001;60:382–7.
[23] Garcia-Martin E, Martinez C, Ladero JM, Gamito FJ, Agundez JA. High frequency of mutations related to impaired CYP2C9 metabolism in a Caucasian population. Eur J Clin Pharmacol 2001;57:47–9.
[24] Loebstein R, Yonath H, Peleg D, Almog S, Rotenberg M, Lubetsky A, et al. Interindividual variability in sensitivity to warfarin-nature or nurture? Clin Pharmacol Ther 2001;70:159–64.
[25] Scordo MG, Aklillu E, Yasar U, Dahl ML, Spina E, Ingelman-Sundberg M. Genetic polymorphism of cytochrome P450 2C9 in a Caucasian and a black African population. Br J Clin Pharmacol 2001;52:447–50.
[26] Stubbins MJ, Harries LW, Smith G, Tarbit MH, Wolf CR. Genetic analysis of the human cytochrome P450 CYP2C9 locus. Pharmacogenetics 1996;6:429–39.
[27] Sullivan-Klose TH, Ghanayem BI, Bell DA, Zhang ZY, Kaminsky LS, Shenfield GM, et al. The role of the CYP2C9-Leu359 allelic variant in the tolbutamide polymorphism. Pharmacogenetics 1996;6:341–9.
[28] Yasar U, Eliasson E, Dahl ML, Johansson I, Ingelman-Sundberg M, Sjoqvist F. Validation of methods for CYP2C9 genotyping: frequencies of mutant alleles in a Swedish population. Biochem Biophys Res Commun 1999;254:628–31.
[29] Korzekwa KR, Krishnamachary N, Shou M, Ogai A, Parise RA, Rettie AE, et al. Evaluation of atypical cytochrome P450 kinetics with two-substrate models: evidence that multiple substrates can simultaneously bind to cytochrome P450 active sites. Biochemistry 1998;37:4137–47.
[30] Egnell AC, Eriksson C, Albertson N, Houston B, Boyer S. Generation and evaluation of a CYP2C9 heteroactivation pharmacophore. J Pharmacol Exp Ther 2003;307:878–87.
[31] Wang RW, Newton DJ, Liu N, Atkins WM, Lu AYH. Human cytochrome P-450 3A4: in vitro drug–drug interaction patterns are substrate-dependent. Drug Metab Dispos 2000;28:360–6.
[32] Egnell AC, Houston JB, Boyer CS. Predictive models of CYP3A4 heteroactivation: in vitro–in vivo scaling and pharmacophore modeling. J Pharmacol Exp Ther 2005;312:926–37.
[33] Maurer TS, DeBartolo DB, Tess DA, Scott DO. Relationship between exposure and nonspecific binding of thirty-three central nervous system drugs in mice. Drug Metab Dispos 2005;33:175–81.
[34] Hunt CA, Jones RT. Tolerance and disposition of tetrahydrocannabinol in man. J Pharmacol Exp Ther 1980;215:35–44.